Journal of Theoretical Biology 595 (2024) 111953

Contents lists available at ScienceDirect

Journal of Theoretical Biology

journal homepage: www.elsevier.com/locate/yjtbi

Optimal resource allocation in micro-organisms under periodic nutrient fluctuations

J. Innerarity Imizcoz [a,*], W. Djema [b], F. Mairet [c], J.-L. Gouzé [a]

[a] Université Côte d'Azur, Inria, INRAE, CNRS, Macbes team, France
[b] Université Côte d'Azur, Inria, Sorbonne Université, CNRS, INRAE, Biocore team, France
[c] Ifremer, PHYTOX, Laboratoire Physalg, France

ARTICLE INFO

Keywords:
Microbial growth
Optimal control
Periodic environment
Pontryagin's Maximum Principle

ABSTRACT

Although microorganisms often live in dynamic environments, most studies, both experimental and theoretical, are carried out under static conditions. In this work, we investigate the issue of optimal resource allocation in bacteria growing in periodic environments. We consider a dynamic model describing the microbial metabolism under varying conditions, involving a control variable quantifying the protein precursors allocation. Our objective is to determine the optimal strategies maximizing the long-term growth of cells under a piecewise-constant periodic environment. Firstly, we perform a theoretical analysis of the resulting optimal control problem (OCP), based on the application the Pontryagin's Maximum Principle (PMP). We determine that the structure of the optimal control must be bang–bang, with possibly some singular arcs corresponding to optimal equilibria of the system. If the control presents singular arcs, then these can only be reached and left through chattering arcs. We also use a direct optimization method, implemented in the BOCOP software, to solve the studied OCP. Our study reveals that the optimal solution over a large time horizon is related to the one over a single period of the varying environment with periodic constraints. Moreover, we observe that the maximal average growth rate attainable under periodic conditions can be higher than the one under a constant environment. We further extend our analysis to conduct a qualitative comparison between the predictions from our model and some recent biological experiments on *E. coli*. This analysis particularly highlights the mechanisms of action of the ppGpp signaling molecule, thus providing relevant explanations of the experimental observations. In conclusion, our study corroborates previous research indicating that this molecule plays a crucial role in the regulation of resource allocation of protein precursors in *E. coli*.

1. Introduction

Bacteria and other microorganisms form the basis of every ecosystem. Also, they play a key role in many bio-industrial processes, such as food and drug production or waste-water treatment (Liao et al., 2016; Yegorov et al., 2019; Yabo et al., 2024). However, important gaps remain in our knowledge of their physiology due to the complexity of studying their internal mechanisms.

Mathematical models have proved to be greatly effective in simplifying the study of bacteria, while being able to reproduce and explain many experimental observations on their growth and metabolism.

Control theory provides a natural tool to approach these problems, which has been applied in a wide variety of biological contexts (Ewald et al., 2017). Using the appropriate objective function, it provides an ideal behavior, and a benchmark for the comparison of other metabolic regulation mechanisms. It is usual to suppose that bacteria are naturally selected to maximize their growth rate, an assumption in accordance with the behavior observed in Edwards et al. (2001) and Ibarra et al. (2002).

Earlier articles investigating the mathematical modelization of the metabolism of microorganisms studied their growth in steady-state conditions (Edwards et al., 2001; Ibarra et al., 2002; Lewis et al., 2010; Scott et al., 2014; Maitra and Dill, 2015). Later studies introduced dynamical modeling of the response of bacteria after a single shift in their environment (Giordano et al., 2016; Pavlov and Ehrenberg, 2013; van den Berg et al., 1998; Yabo et al., 2022; Ehrenberg et al., 2013; Yegorov et al., 2019; Waldherr et al., 2015). These have been significant steps in the study of the mechanism of the optimization of resource allocation in micro-organisms. However, the type of conditions that these models represents is only in accordance with what microorganisms can face in a laboratory, where it is feasible to maintain a constant environment (Borirak et al., 2014).

* Corresponding author.
E-mail address: javier.innerarity-imizcoz@inria.fr (J. Innerarity Imizcoz).

https://doi.org/10.1016/j.jtbi.2024.111953
Received 13 May 2024; Received in revised form 12 September 2024; Accepted 19 September 2024
Available online 30 September 2024

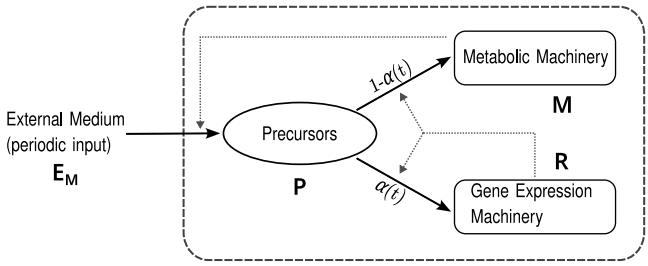

Fig. 1. Diagram of our model of bacterial metabolism. The control variable α represents the proportion of protein precursors allocated to producing R. The environment E_M is a piecewise-constant period input.

In a natural setting, it is not reasonable to assume that the environment of a given individual remains constant. We must therefore consider time-dependent environments if we want to study the mechanisms regulating the allocation of its resources in a more realistic context (Nguyen et al., 2021a).

For this reason, we modify the resource allocation model proposed in Giordano et al. (2016) by setting the substrate availability in the environment of a given cell to a periodic piecewise-constant function. This results in a more realistic environmental input, representing the cyclic changes in substrate concentration that are caused for example by day–night dynamics or for host-associated microbes by periodic feeding of the host.

One of the main results of this work is showing that there exists a non-constant periodic environment which improves on the maximal average growth rate attainable in a constant medium. We also find that the mechanism of regulation induced by the ppGpp molecule explains well the behavior of bacteria in dynamic environments. This nucleotide has been found to play a crucial role in bacterial response to changes in amino acid concentration by downregulating rRNA synthesis (Potrykus and Cashel, 2008; Magnusson et al., 2005).

The paper is organized as follows. We introduce the model of interest in Section 2, where the environment is non-constant. Then, we state the optimal control problem (OCP) in Section 3. We address this OCP through the application of a variant of Pontryagin's Maximum Principle (PMP) in Section 4. Next, we numerically obtain the solution of the problem in Section 5. Section 6 is devoted to studying the relationship between the infinite-time OCP and the problem with periodic boundary conditions of the same period as the environment. In Section 7, we study how two key parameters of the environment, its period and amplitude, affect the solution of the OCP. Finally, we study the ppGpp-regulated suboptimal strategy, which we compare with the optimal control and with experimental observations on *E. coli* (Nguyen et al., 2021b) in Section 8.

2. The mathematical model

We modify the self-replicator model proposed in Giordano et al. (2016), which represents the metabolism of a given micro-organism. The external medium (E_M) of this cell has some substrate that the cell can absorb and convert into precursor metabolites (P) through some reactions catalyzed by the metabolic machinery (M). These precursors are then converted by the gene expression machinery (R) into the macromolecules that form R and M. The resource allocation parameter $\alpha(t)$ is the proportion of the precursor's mass used to build R at a given time t. This process is schematized in Fig. 1.

The model can be simplified by dividing all the variables by the total volume of the cell, which is assumed to be proportional to the total macromolecular mass, $V = \beta(M + R)$, with $\beta > 0$. We also suppose that reactions follow Michaelis–Menten dynamics. After normalization, the system reads as follows.

$$\begin{cases} \dot{p} &= (1-r)E_M(t) - (1+p)\frac{p}{K+p}r \\ \dot{r} &= (\alpha - r)\frac{p}{K+p}r \\ \dot{V} &= \frac{pr}{K+p}V, \end{cases} \tag{1}$$

where p and r are time-dependent variables. The first one represents the cytoplasmic concentration of P, whereas r is the concentration of R. The concentration of M does not need to appear in these equations as it can be defined by $m = 1 - r$. The resource allocation parameter $\alpha(t)$ will be the control exerted on the system. The parameter K is intrinsic to the metabolism of the cell, and will therefore be treated as a constant. In Giordano et al. (2016) the parameter E_M, representing the richness of the external medium (summing up a Michaelis Menten function of the substrate), is considered to be constant.

We propose to modify this system by setting E_M to be a piecewise-constant periodic input of period $T > 0$, described by

$$E_M(t) = \begin{cases} E_M^{\max}, & \text{if } t \in [0, T/2), \\ E_M^{\min}, & \text{if } t \in [T/2, T), \end{cases} \tag{2}$$

with $0 < E_M^{\min} < E_M^{\max}$. This definition of E_M yields a more realistic model, which takes into account the always-changing conditions in which microorganisms usually grow. These conditions nevertheless tend to exhibit some kind of periodic behavior. For example, one can think of ecosystems in which the substrate availability is dependent on the amount of sunlight it receives (Mairet and Bayen, 2021).

3. Statement of the dynamic optimal control problem

We seek to determine the resource allocation strategy that will maximize the volume increase of the cells. We define the quantity

$$\mu(t) = \frac{pr}{K+p}(t),$$

which is the growth rate of the cell. That is,

$$V(t) = V(0)\exp\int_0^t \mu(\tau)\, d\tau \ \forall t \geq 0. \tag{3}$$

Therefore, maximizing is equivalent to maximizing

$$\int_0^t \mu(\tau)\, d\tau.$$

Here, we seek the strategy that is able to optimize growth on an infinite time-interval, *i.e.* we are interested in the optimal long-term strategy. The objective of our optimal control problem (OCP) is thus to find

$$\alpha_{opt} \text{ such that } \liminf_{t_f \to \infty} \left(J_{t_f}(\alpha_{opt}) - J_{t_f}(\alpha) \right) \geq 0 \ \forall \alpha \in U_\infty,$$

where

$$J_{t_f}(\alpha) = \int_0^{t_f} \frac{pr}{K+p}\, dt,$$
$$U_\infty = \{\alpha : [0, +\infty) \to [0,1] \mid \alpha \text{ is measurable}\}$$

and the system $(p, r, V)(t)$ follows System (1). Note that, since p and r are independent from the cellular volume V, we can omit this last variable from System (1).

We will start our study of the OCP by carrying out its theoretical analysis in the following section.

4. Application of Pontryagin's Maximum Principle

4.1. Optimality conditions

For the theoretical analysis of the optimization problem, we will use the Infinite Horizon Maximum Principle (Carlson et al., 2012), an

extension of Pontryagin's Maximum Principle (PMP), which includes most of its results. We set the Hamiltonian

$$\begin{aligned} H &= H(p,r,\lambda_p,\lambda_r,\lambda_0,\alpha,t) = \lambda_p\dot{p} + \lambda_r\dot{r} + \lambda_0\left(\frac{pr}{K+p}\right) \\ &= \lambda_p\left[(1-r)E_M(t) - \frac{(1+p)pr}{K+p}\right] + \lambda_r\frac{(\alpha-r)pr}{K+p} + \lambda_0\frac{pr}{K+p} \\ &= H_0 + H_1\alpha, \end{aligned}$$

where

$$H_0 = \lambda_p\left[(1-r)E_M(t) - (1+p)\frac{pr}{K+p}\right] - \lambda_r\frac{pr^2}{K+p} + \lambda_0\frac{pr}{K+p}$$

, and

$$H_1 = \lambda_r\frac{pr}{K+p}.$$

The adjoint variables fulfill $(\lambda,\lambda_0) = (\lambda_p,\lambda_r,\lambda_0) \neq 0$, $\lambda_0 \geq 0$ and the differential equations

$$\begin{cases} \dot{\lambda}_p &= \lambda_p\frac{r(2Kp+K+p^2)}{(K+p)^2} + \lambda_r(r-\alpha)\frac{Kr}{(K+p)^2} - \lambda_0\frac{Kr}{(K+p)^2} \\ \dot{\lambda}_r &= \lambda_p\left[E_M(t) + \frac{(1+p)p}{K+p}\right] + \lambda_r\frac{p(2r-\alpha)}{K+p} - \lambda_0\frac{p}{K+p}. \end{cases} \tag{4}$$

We also have the maximization condition

$$H(t,p,r,\lambda,\lambda_0,\alpha(t)) = \max_{v\in[0,1]} H(t,p,r,\lambda,\lambda_0,v) \text{ a.e. on } [0,+\infty).$$

Finally, the Hamiltonian obeys the differential equation

$$\frac{dH}{dt} = \frac{\partial H}{\partial t} = \lambda_p(1-r)\frac{dE_M}{dt}(t) \text{ a.e.,} \tag{5}$$

which implies that H remains constant when E_M is also constant.

4.2. Analysis of optimal controls

The above conditions allow to find the possible values of α_{opt}, which are given in Theorem 4.1.

Theorem 4.1. *The optimal control α_{opt} is given by*

$$\alpha_{opt}(t) = \begin{cases} 1 \text{ if } \lambda_r > 0 \\ 0 \text{ if } \lambda_r < 0 \\ \alpha^*_{opt}(E_M(t)) \text{ if } \lambda_r = 0, \end{cases}$$

where

$$\alpha^*_{opt}(E_M) = \frac{E_M + \sqrt{KE_M}}{E_M + 2\sqrt{KE_M} + 1}.$$

If $\lambda_r = 0$ on a time interval $t \in [t_1,t_2]$, with $t_1 < t_2$, the system must lie at the equilibrium point $(p^*_{opt},r^*_{opt})(E_M(t))$, where

$$p^*_{opt}(E_M) = \sqrt{KE_M} \text{ and } r^*_{opt}(E_M) = \alpha^*_{opt}(E_M). \tag{6}$$

Proof. Since the control is affine in α, and by the maximization condition on H, we have that α_{opt} takes its maximal (resp. minimal) value when $H_1 > 0$ (resp. $H_1 < 0$). By the positivity of p and r, the sign of H_1 is simply the same as λ_r.

If the optimal control has a singular arc (a time interval $t \in [t_1,t_2]$, with $t_1 < t_2$, over which $\lambda_r = 0$), then λ_0 must be non-zero and we can normalize the adjoint variables by setting $\lambda_0 = 1$. Indeed, if it were $\lambda_0 = 0$, then on the singular arc

$$0 = \dot{\lambda}_r = \lambda_p\left[E_M(t) + \frac{(1+p)p}{K+p}\right] \implies \lambda_p = 0 \implies (\lambda,\lambda_0) = 0,$$

which contradicts the optimality conditions.

Therefore, over the singular arc,

$$\begin{cases} H = \lambda_p\left[(1-r)E_M(t) - \frac{(1+p)pr}{K+p}\right] + \lambda_0\frac{pr}{K+p} \\ \dot{\lambda}_r = \lambda_p\left[E_M + \frac{(1+p)p}{K+p}\right] - \lambda_0\frac{p}{K+p} = 0, \end{cases}$$

which implies that, in a singular trajectory,

$$H = \lambda_p E_M(t).$$

Let $t_s \in [t_1,t_2]$ be a time point different from the discontinuities in E_M. By (5), and since E_M is locally constant around t_s, so is H. Therefore, by the above equation, the adjoint variable λ_p must also be locally constant. By combining the equations $\dot{\lambda}_r = 0$ and $\dot{\lambda}_p = 0$, we obtain that $p = p^*_{opt}(E_M)$, given by Eq. (6).

In particular, p is locally constant around t_s and the equation $\dot{p} = 0$ yields $r = r^*_{opt}(E_M)$. Since $r(t)$ is locally constant we must have that $\alpha = r = \alpha^*_{opt}(E_M)$. Since the points $(p^*_{opt},r^*_{opt})(E_M)$ are different between two different values of E_M, a singular arc cannot contain the discontinuities of E_M, as it would require a discontinuity in the system. □

We have just proved that singular arcs in a piece-wise constant environment correspond to intervals on which the system is constant. In the following subsection, we will see that this constant value is precisely the equilibrium point that optimizes steady-state growth.

4.3. Relation to the static OCP

We seek to understand why the singular arcs of the optimal control correspond to such concrete static values of the system. In order to do so, we focus on the static OCP of finding which of these equilibrium points yields the highest growth rate. That is, for a given constant value of E_M, we seek to determine the tuple

$$(\alpha^*,p^*,r^*) \in [0,1]\times\mathbb{R}^+\times[0,1]$$

such that

$$\begin{cases} (\dot{p},\dot{r})(\alpha^*,p^*,r^*) = 0 \\ \mu^*(\alpha^*,p^*,r^*) = \frac{p^*r^*}{K+p^*} \text{ is maximal.} \end{cases}$$

For each possible value of $E_M > 0$, this problem admits only one solution (see Giordano et al. (2016)), which is precisely the tuple $(\alpha^*_{opt},p^*_{opt},r^*_{opt})(E_M)$ given by Theorem 4.1. Therefore, we reinterpret the theorem as follows. The optimal control must take its maximal or minimal value, except when the system lies at its optimal equilibrium point. In the following, we shall call the optimal steady-state growth rate $\mu^*_{opt} = \frac{p^*_{opt}r^*_{opt}}{K+p^*_{opt}}$.

4.4. The Kelley condition and chattering phenomena

To check whether a singular arc of the system verifies the Kelley Condition (Marchal, 1973), we compute the derivatives

$$\frac{\partial}{\partial\alpha}\frac{d^k}{dt^k}H_1$$

over a singular arc. They are null for all $k < 4$. For q=2, we find

$$\frac{\partial}{\partial\alpha}\frac{d^{2q}}{dt^{2q}}\phi(t) = -\frac{p^2r^2\left[2pE_M(t) + (K+2p)E'_M(t)\right]}{(K+p)^4}.$$

Since singular arcs of our control are contained in intervals over which E_M is constant, the necessary condition to have a singular trajectory

$$(-1)^q\frac{\partial}{\partial\alpha}\frac{d^{2q}}{dt^{2q}}\phi(t) < 0,$$

is fulfilled over any singular arc. This arc is of even order $q = 2$, which means that it can only be attained and left through chattering (Borisov, 2000). That is, in order to attain the singular arc, an infinite amount of bang arcs are needed in a finite time.

We have found that the optimal control consists of a concatenation of bang arcs, with possibly some singular arcs corresponding to the solution of the related static optimization problem. If these singular arcs appear, they can only be reached and left through chattering. In the next section, we will solve the OCP numerically, which will shed more light on the structure of the optimal control.

Table 1
Conditions of the numerical resolution.

K	$E_M^{\min}$	$E_M^{\max}$	T	(p_0, r_0)
0.003	0.2	1.0	10	(0.024, 0.18)

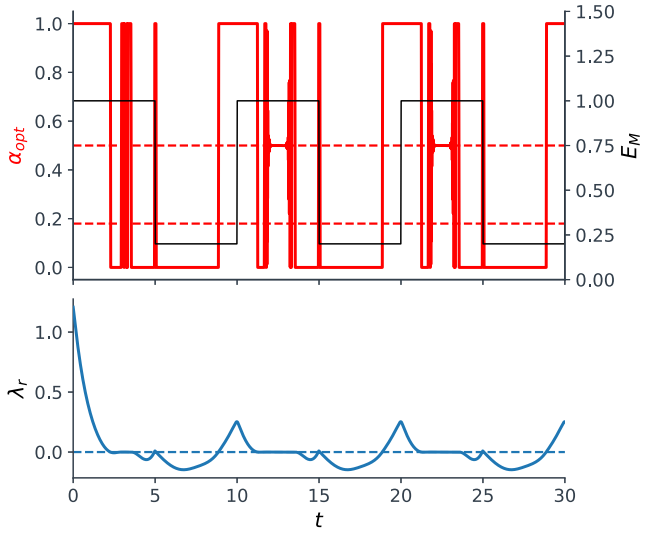

Fig. 2. Result of the numerical simulation of the OCP for a finite final time of $t_f = 40$. The plots over the last period have been omitted. On the top subfigure, the optimal control. The top dotted line corresponds to $\alpha^*_{opt}(E_M^{\max})$ and the bottom one to $\alpha^*_{opt}(E_M^{\min})$. In a black thinner line, the environmental input E_M. On the bottom, the time plot of λ_r. The sign of this adjoint variable determines the value of α_{opt}. The intervals on which λ_r is zero correspond to the singular arcs of α_{opt}.

5. Numerical computation of the optimal control

We now compute the optimal control by means of a direct numerical resolution, that is we discretize the system of ODEs. We set a finite time horizon of $t_f = 40 = 4T$. We will omit the last period of the result, as the control will be seen to tend to a limit cycle, before changing on this last period due to boundary effects and thus depleting the cell of a great part of its precursor resources p a short time before the final time of the simulation. We will see in Section 6 that this limit cycle is the solution of the similar optimization problem of maximizing growth over one period with periodic boundary conditions.

The values of the constant and initial values of the OCP fed into the optimal control solver BOCOP (Inria Saclay Team Commands, 2017) are given in Table 1. The initial value of the system corresponds to $(p_0, r_0) = (p^*_{opt}, r^*_{opt})(E_M^{\min})$. This point corresponds to the steady-state optimal for $E_M = E_M^{\min}$, which has been found in Lewis et al. (2010) to be the point naturally attained by bacteria in constants environments. The structure of the optimal control described in Section 5.2 remains similar for the different initial conditions that we have tested. We have used $N = 4000$ time steps and a relative tolerance of 10^{-14}.

5.1. Result of the numerical resolution

The top plot of Fig. 2 shows the optimal control α_{opt} found for this piece-wise constant periodic environment. We see from the plot that the optimal control seems to tend to a limit cycle. We are able to numerically verify this convergence. Because of this limit cycle, and since the last period is affected by the proximity of the final time of the resolution, we have decided to plot α_{opt} only until the time $t = 30 = 3T$.

5.2. Structure of the optimal control

The optimal control starts with a first transient phase on the interval $[0, T]$ and then becomes periodic, with the same period as E_M. During its first period, it presents a very brief constant singular arc included in the interval over which the environmental variable is maximal. This singular arc is longer during the phase where α_{opt} becomes periodic. In both cases, the singular arc is preceded and followed by bang–bang arcs, with chattering occurring in between. This is in accordance with the theoretical study carried out in Section 4.

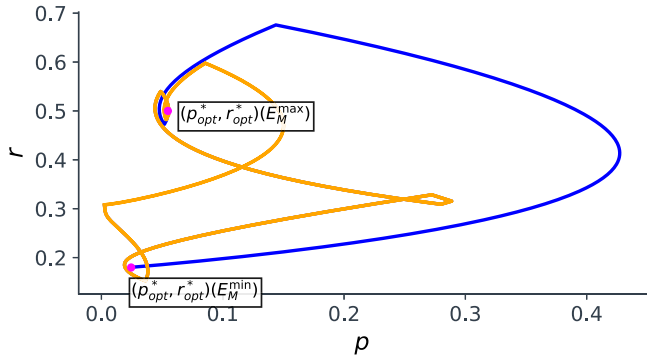

Fig. 3. Phase plot of the variables p and r from (1), on the time-interval $[0, 3T]$ and under α_{opt}. In blue, over the first period and in orange over the second and third periods (which are overlapped). The solutions of the static OCP corresponding to both possible values of E_M are highlighted.

We notice that the control does not reach the second theoretically possible singular arc, which would correspond to $E_M = E_M^{\min}$. However, if the period is long enough, the control does reach both possible singular arcs. It may also have no singular arcs (see Fig. 5) if the period is short enough. We have seen in Subsection Section 4.3 that, during its singular phase, the solution of the dynamic OCP converges toward that of the static OCP, as previously observed in this class of systems when E_M is constant (see, e.g., citecaillau2022turnpike and references therein). This turnpike phenomenon Trélat (2023) is well-known and has been observed in various similar problems in biology Caillau et al. (2022), Djema et al. (2021, 2022). In this case we observe the emergence of a turnpike with different values, each of these corresponding to a different value of the environmental input.

The bottom plot of Fig. 2 shows the time plot of the adjoint variable λ_r, obtained through the resolution of System (4). This variable determines the value of α_{opt}. From this plot, we confirm that λ_r is null on the computed singular arcs. As happens to the control, the system goes through a transient first period to then become periodic, as shown in Fig. 3. As mentioned previously, the point $(p^*_{opt}, r^*_{opt})(E_M^{\max})$ is reached during this periodic phase, but not $(p^*_{opt}, r^*_{opt})(E_M^{\min})$.

5.3. Feasibility of the optimal strategy

We also notice that the control anticipates the changes in the environment of the bacteria, by having a bang arc $\alpha = 1$ or $\alpha = 0$ which begins shortly before a discontinuity in E_M. This increases the concentration of gene expression machinery (r) to prepare for a higher concentration of nutrients (given by a higher E_M), or decreases r in preparation for the upcoming nutrient shortage. This property is consistent with what has been found in other biological OCP in the literature (Mairet and Bayen, 2021).

One may wonder about how this particular aspect of the optimal control can be implemented in practice, as it requires knowledge of the future evolution of the environment of the cell. We can make the supposition that bacteria are specially prepared to thrive in an environment with a certain period. One can think for example of how day/night (Muratore et al., 2022) or seasonal dynamics all have a fixed period. We shall also see in Section 8 how a simple feedback control independent from E_M can result in near-optimal growth.

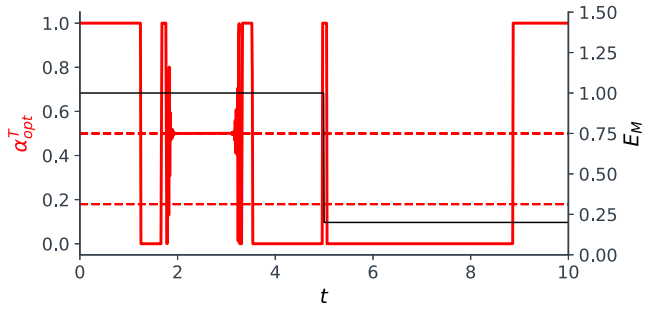

Fig. 4. The optimal control for the periodic problem. Its plot coincides visually with that of the optimal control for the original problem over $t \in [2T, 3T)$.

6. Relation to the periodic problem

In Giordano et al. (2016), it is shown that the optimal control (in a static environment) ended in a constant arc corresponding to a stable equilibrium point that maximized steady-state growth. In the case of a periodic environment, the equivalent of an equilibrium point under a constant control is a periodic orbit corresponding to a periodic control. We would like to investigate which control maximizes growth on such an orbit of the same period as the environment, and whether the optimal control that we found in Section 5 tends to it.

That is, we are now interested in solving the similar problem of finding a control

$$\alpha^T_{opt} \in \arg\max \int_0^T \frac{p}{K+p} r \, dt,$$

where the system $(p, r)(t)$ follows System (1) and fulfills the periodic boundary condition $(p, r)(T) = (p, r)(0)$. The environment is given, as stated above, by Eq. (2).

The solution to this problem is shown in Fig. 4. This control and the optimal control for our initial problem (on the limit cycle shown in Fig. 2) completely overlap. This seems to be a general phenomenon associated with our model, irrespective of the parameters used. We see that in a periodic environment the infinite-horizon optimal control eventually leads the system along a periodic trajectory which is optimal along the set of all periodic trajectories of the same period T.

7. Effect of the period and amplitude of the environment

In this section, we will study how two of the parameters defining the environment given by (2) affect the resulting long-term volume increase of the solution of our OCP. We will consider a fixed average environmental capacity, defined as

$$\overline{E}_M = \frac{1}{T} \int_0^T E_M(t) \, dt.$$

For the environmental input defined in Eq. (2), we have that $\overline{E}_M$ is the arithmetic mean of $E_M^{\min}$ and $E_M^{\max}$.

The parameters whose effect we will study are the period T and the amplitude of the environment $\Delta E_M = E_M^{\max} - E_M^{\min}$. Thus, we can define the environmental input E_M by giving, instead of its two possible values, its average and its amplitude. The condition that $E_M^{\min}$ be positive is equivalent to $\Delta E_M \leq 2\overline{E}_M$.

In order to measure the asymptotic volume increase rate, we will use the equivalent average growth rate over a period of the limit cycle. This rate can be defined over any time interval $[0, t]$ as

$$\overline{\mu}(t) = \frac{\log(V(t)) - \log(V(0))}{t} = \frac{\int_0^t \mu(\tau) d\tau}{t},$$

such that $V(t) = V(0)e^{\overline{\mu}(t)t}$. If, as we will do in this section, we focus on $\overline{\mu}(T)$, the average growth rate over a period of duration T of the environmental input, we obtain that $V(t)$ behaves asymptotically as $e^{\overline{\mu}(T)t}$. We will take $V(t)$ to be the volume variable of the solution to the problem defined in Section 6.

It is especially interesting to investigate whether, for a fixed $\overline{E}_M$, there exist some T and ΔE_M that maximize the average exponential increase in biomass that the solution of the optimal control problem with those parameters yields. If this is so, we would want to approximate those values and measure how much it increases the potential cell growth with respect to the one attainable in a constant environment.

We will use the BOCOP solver to find the value of the parameters T and ΔE_M that maximize this average growth $\overline{\mu}(T)$ over a period, assuming the control $\alpha = \alpha^T_{opt}$ defined in Section 6, which depends on T and on ΔE_M. In order to be able to include T into the differential equations system we normalize by dividing the time by this parameter so that the normalized system reads as follows.

$$\begin{cases} \frac{dp}{d\hat{t}}(\hat{t} = t/T) &= T\left[(1-r)E_M(\hat{t}) - (1+p)\frac{p}{K+p}r\right] \\ \\ \frac{dr}{d\hat{t}}(\hat{t} = t/T) &= T\left[(\alpha - r)\frac{p}{K+p}r\right], \end{cases}$$

where the environmental constant with normalized time is given by

$$E_M(\hat{t}) = E_M(t) = \begin{cases} E_M^{\max}, & \text{if } t \in [0, T/2) \iff \hat{t} \in [0, 1/2) \\ E_M^{\min}, & \text{if } t \in [T/2, T) \iff \hat{t} \in [1/2, 1) \end{cases}$$

and the periodic conditions are now

$$\begin{cases} p(\hat{t} = 1) &= p(\hat{t} = 0) \\ r(\hat{t} = 1) &= r(\hat{t} = 0) \end{cases}$$

The average growth rate $\bar{\mu}(T)$ to be maximized can be expressed as a function of the variables in normalized time as

$$\bar{\mu}(T) = \int_0^1 \frac{pr}{K+p}(T\hat{t}) d\hat{t}.$$

As before, we take the constants $K = 0.003$ and $\overline{E}_M = 0.6$ for the numerical resolution of this problem. We now seek to optimize over three variables: the resource allocation parameter $\alpha : [0, +\infty) \to [0, 1]$ and the real parameters $T \in (0, +\infty)$ and $\Delta E_M \in [0, 2\overline{E}_M]$.

When initialized with the right initial conditions, the BOCOP software (Inria Saclay Team Commands, 2017) gives a solution of $(T, \Delta E_M) \approx (0.26, 1.2 = 2\overline{E}_M)$, which results in an average growth rate of $\overline{\mu}_{opt} \approx 0.3571$, slightly better than in a constant environment ($\mu^*_{opt} \approx 0.3561$). Note that the optimal amplitude of the environment appears to be the maximal possible one. The optimal control for this environment, which is plotted in Fig. 5, has a simple bang–bang structure, with just two switches per period.

Even though it only slightly enhances the maximal growth rate attainable in a constant environment, this result is in our opinion very interesting, as it shows that it is possible to have periodic conditions which are more advantageous than constant ones. This result has been proved in the literature for other biological process (Silveston et al., 2008), but it is not generally true that periodic inputs improve on constant ones (Ali Al-Radhawi et al., 2021).

We shall see in the following section how our model explains some of the behaviors actually observed in real-life bacteria.

8. Study of a control strategy

In this section, we will study one control strategy that appears to be the one naturally used by real-life bacteria. The ppGpp signaling molecule has been found to play an important role in the regulation of the transcription of growth-related genes (Potrykus et al., 2011; Gaca et al., 2015; Liu et al., 2015). Following our assumption that bacteria are selected by evolutionary pressure according to their ability to outgrow their opponents, we will see how the α determined by the mechanisms of ppGpp compares to the optimal control in terms of resulting growth rate in a periodically changing environment. This

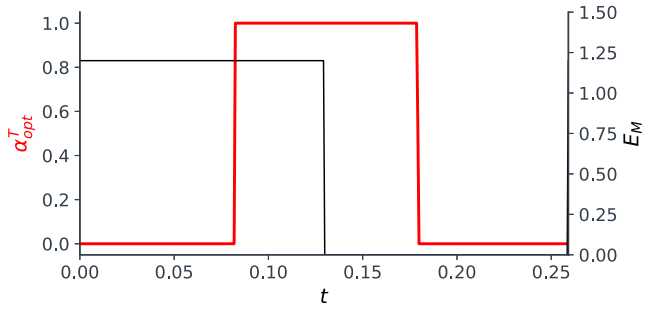

Fig. 5. Plot of the optimal control α^T_{opt} for the environmental input defined by Eq. (2) with the optimal parameters $(T, \Delta E_M) \approx (0.26, 1.2 = 2\overline{E}_M)$.

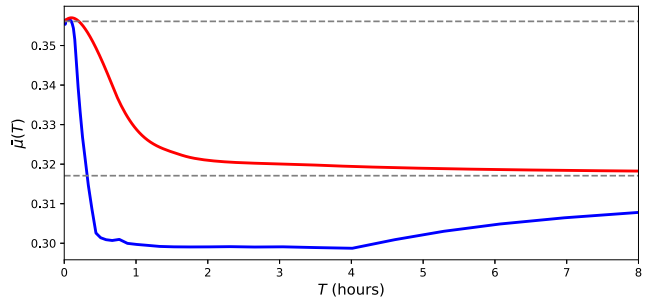

Fig. 6. Average growth rate on a period of the limit cycle, under the optimal α (red) and the on–off control (blue). The top dotted line corresponds to μ^*_{avg} and the bottom one to μ_J.

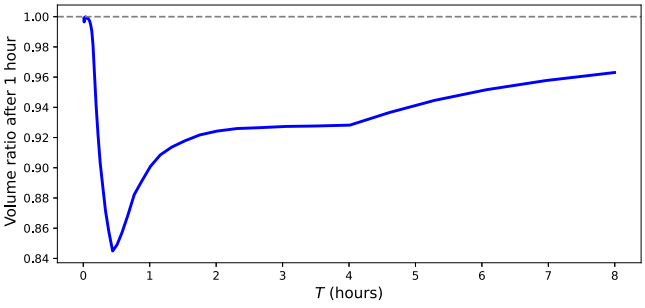

Fig. 7. Ratio between the cellular volumes after one hour on the limit cycle, under the on–off control and under the optimal control.

suboptimal control strategy was found in Giordano et al. (2016) to result in a near-optimal growth when the bacteria were exposed to a single upshift in the concentration of nutrients.

We will also compare the experimental observations realized on bacteria evolving in fluctuating environments (Nguyen et al., 2021b) to the ones that can be drawn from our model, assuming the cell population implements this ppGpp-mediated strategy in all types of environment. These comparisons will yield insights on the importance of this molecule in regulating the response of bacteria to fluctuations in their environment.

8.1. Optimality of ppGpp

We now compare the growth rate attained using the optimal control and the ppGpp-regulated one. We consider the on–off control given in Giordano et al. (2016), which is found in that same article to be very similar to the actual functioning of the ppGpp molecule.

This on–off control is given by

$$\alpha = \begin{cases} 1 & \text{if } r < g(p) \\ 0 & \text{if } r > g(p) \\ r & \text{if } r = g(p) \end{cases},$$

where

$$g(p) = \frac{p^2 + Kp}{p^2 + 2Kp + K},$$

so that

$$g(p^*_{opt}(E_M)) = r^*_{opt}(E_M)\ \forall E_M \geq 0.$$

Thus, for a constant E_M, the system under this control has $(p^*_{opt}, r^*_{opt})(E_M)$ as a globally asymptotically stable equilibrium point. This implies that the rate $\bar{\mu}(T)$ of bacteria under this on–off control tends to μ_J, the mean between $\mu^*_{opt}(E^{\max}_M)$ and $\mu^*_{opt}(E^{\min}_M)$, when T grows to infinity.

In order to find the theoretically optimal behavior of bacteria accustomed to a periodic environment, we take the solution α^T_{opt} to the problem defined in Section 6, which we have shown in that section to correspond to the limit cycle of the infinite-horizon optimal control. For simulating the on–off strategy, we have numerically computed its limit cycle.

We have solved the resulting optimal control problems using BOCOP, with the same parameters as in Table 1, except for the period T and the boundary conditions.

For a large range of values of T, we have calculated the average growth rate on a given period $\bar{\mu}(T)$ under the optimal and the on–off control. We have compared both average rates with each other and with μ^*_{avg}, the optimal steady-state growth rate in a constant environment $E^{\text{avg}}_M = (E^{\max}_M + E^{\min}_M)/2$. The results are shown in Fig. 6. We can appreciate how the average growth rate under the optimal control tends to μ_J, as it does under the on–off control. This is due to the fact that α^T_{opt} tends to spend most of each subperiod on the singular arc corresponding to $(p^*_{opt}, r^*_{opt})(E_M)$. This property has also been observed in the optimal control after a single shift in the environment in Giordano et al. (2016), and is in accordance with the findings of Edwards et al. (2001), Ibarra et al. (2002) on the behavior of bacteria in steady environments.

Neither the optimal strategy nor the on–off control show a decrease in the obtainable growth rate with respect to a constant medium for the most rapidly varying periodic environments. For longer periods T, we observe that the growth rate becomes significantly smaller, although this difference is more pronounced in the case of the on–off control.

Fig. 7 shows the volume loss per hour of a cell using the ppGpp-regulated control when compared to a cell that uses the optimal control. The former control strategy is close to optimal for very short or long periods T, although it shows a significant loss in growth rate for periods ranging from a dozen minutes to an hour. It can lose up to 15% of mass every hour when compared to an optimal strategy for a period T of approximately 30 min. This may result from an evolutionary adaptation to either fast or slow adaptations, or from an intrinsic difficulty in adapting to fluctuating environments of an intermediate period. Future experiments on bacterial evolution in dynamical conditions may shed more light on this matter.

8.2. Comparison with experimental data

We now compare some of the theoretical results that can be obtained through our model to the ones directly measured on *E. coli* in Nguyen et al. (2021b). In the series of experiments described in that article, some of the microorganisms are kept in a constant environment (corresponding to $E_M = E^{\max}_M$ or $E_M = E^{\min}_M$ in our model) and others evolve in a fluctuating environment which follows the same piecewise-constant periodic shape as our E_M. These last bacteria are divided into groups for which the environment is of period T = 30 s, 5, 15 or 60 min. When a periodic regime is achieved, the resulting growth rate is measured by single-cell microscopy and compared to a single shift experiment.

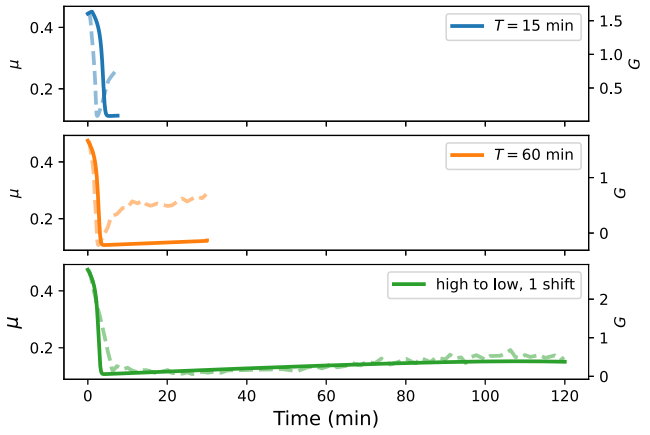

Fig. 8. Time plot of the growth rate $\mu(t)$ in a downshift scenario and under an on–off control $\alpha = \alpha(p, r)$. Dotted lines indicate experimental data.

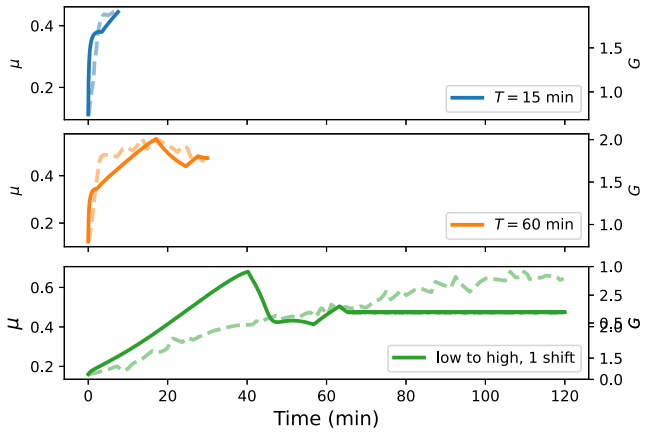

Fig. 9. Time plot of the growth rate $\mu(t)$ in an upshift scenario and under an on–off control $\alpha = \alpha(p, r)$. Dotted lines indicate experimental data.

We have also simulated the reaction (in terms of the time-evolution of their growth rate μ) to a single upshift or downshift of bacteria previously evolving in a constant poor or rich environment, respectively. The initial conditions for these simulations are therefore $(p_0, r_0) = (p^*_{opt}, r^*_{opt})(E_M^{\min})$ or $(p_0, r_0) = (p^*_{opt}, r^*_{opt})(E_M^{\max})$ for bacteria accustomed to a (constant) low or rich environment, respectively. We have then compared it with the response to the same scenarios of bacteria acclimatized to periodic environments, that is on the limit cycle produced by the on–off control and their respective environment E_M. Figs. 8 and 9 summarize the results obtained. We have plotted the growth rate on a long, 2 h time span for cells used to a constant environment, and on one semi-period of time length $T/2$ (the interval $[0, T/2]$ in the case of an upshift and $[T/2, T]$ in the case of a downshift) for the other bacteria, as has been done in Nguyen et al. (2021b).

The on–off control produces a sharper increase in growth rate immediately after the upshift in bacteria dwelling in periodic environments in comparison to a single upshift, as shown in Fig. 9. This behavior can also be seen in the experimental data shown in the same plots. It has led the authors of Nguyen et al. (2021b) to propose that the mechanisms regulating bacterial growth may be different between constant and periodic environments. In a downshift scenario, the on–off strategy exhibit a very similar behavior in all conditions (Fig. 8).

One may wonder why the same on–off control yields different growth rates in bacteria previously dwelling in different environments. The answer is that the differential equations system has different limit cycles depending on the period of E_M, as can be seen in Fig. 10.

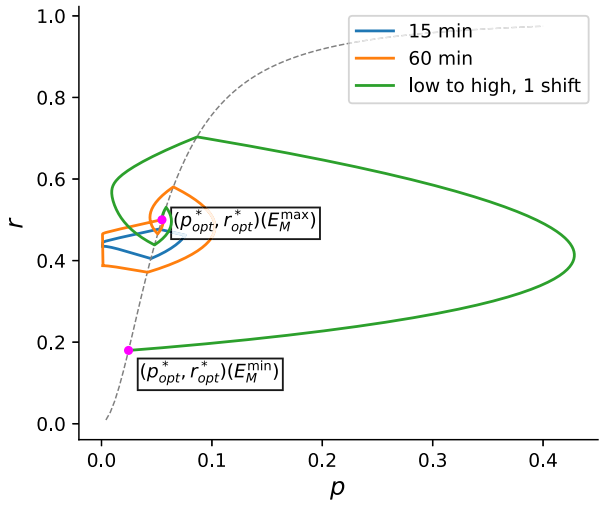

Fig. 10. Different limit cycles of the system under the on–off control corresponding to different values of the environmental period T. The dotted line corresponds to $r = g(p)$, the switch in α. The equilibrium points corresponding to $E_M^{\max}$ and $E_M^{\min}$ are also marked.

None of the cycles studied in this article attain the equilibrium points $(p^*_{opt}, r^*_{opt})(E_M^{\min})$ and $(p^*_{opt}, r^*_{opt})(E_M^{\max})$, the starting points of the simulations for the bacteria previously in a constant environment. The difference in the time-evolution of the growth rates is thus explained by the difference in the starting points of the system.

In conclusion, the on–off feedback strategy, which we remind the reader is similar to the actual dynamic of the ppGpp signaling molecule, appears to explain well the differences observed in Nguyen et al. (2021b) between bacteria accustomed to a constant environment and those evolving in a periodic one. In addition, the growth rate attainable under this control is close to the maximal theoretically possible one. This corroborates previous findings (Potrykus et al., 2011; Gaca et al., 2015; Liu et al., 2015) highlighting the crucial role the ppGpp signaling molecule plays in the regulation of the allocation of protein precursors in *E. coli*.

9. Conclusion

In this work, we studied the problem of the optimization of resource allocation in bacteria in a dynamic environment. Basing ourselves on the model proposed in Giordano et al. (2016), we modified the input representing the substrate availability to a periodical one, which is better able to capture the real-life conditions of most microorganisms.

We gave a precise definition of our optimal control problem, and carried out a theoretical study of its solution using a variant of Pontryagin's Maximum Principle.

We proved, using this theorem, that the optimal infinite-horizon control follows a bang–bang structure, with two possible distinct singular arcs. We saw that each of these arcs corresponds to a steady-state which is the solution of the related static OCP. In addition, we demonstrated that singular arcs can only be reached and left through chattering.

We then computed this optimal control numerically, using the BOCOP software. We saw how, for the set of parameters that we used, the control goes through a transient phase before repeating the solution of the related periodic problem at infinity. These numerical computations also showed how, in periodic environments, the optimal control strategy requires microorganisms to anticipate the changes in the environment. Additionally, we found, among all environments of the same shape and given mean, the one that resulted in the highest optimal growth rate.

Finally, we considered a control strategy that is likely the one implemented by real-life bacteria. We compared the average growth-rate

produced by the ppGpp-mediated control to the solution of the OCP. We also compared the time evolution of growth rate of bacteria that use this suboptimal control with the one measured experimentally. Through these simulations, we have found strong evidence that corroborate that the ppGpp signaling molecule regulates the protein resource allocation in *E. coli*.

CRediT authorship contribution statement

J. Innerarity Imizcoz: Writing – original draft, Software, Methodology, Formal analysis, Conceptualization. **W. Djema:** Supervision, Methodology, Formal analysis, Conceptualization. **F. Mairet:** Supervision, Methodology, Formal analysis, Conceptualization. **J.-L. Gouzé:** Supervision, Methodology, Formal analysis, Conceptualization.

Declaration of competing interest

The authors declare that they have no known competing financial interests or personal relationships that could have appeared to influence the work reported in this paper.

Acknowledgments

This work has been supported by the French government, through the EUR DS4H Investments in the Future Project managed by the National Research Agency (ANR) with the reference number ANR-l7-EURE-0004, and also as part of the Initiative of Excellence Université Côte d'Azur under reference number ANR-15-IDEX-01. It was also partially supported by ANR project Ctrl-AB (ANR-20-CE45-0014) and Labex SIGNALIFE (ANR-11-LABX-0028-01).

References

Ali Al-Radhawi, M., Margaliot, Michael, Sontag, Eduardo D., 2021. Maximizing average throughput in oscillatory biochemical synthesis systems: an optimal control approach. Royal Soc. Open Sci. 8 (9), 210878.

Borirak, Orawan, Bekker, Martijn, Hellingwerf, Klaas J., 2014. Molecular physiology of the dynamic regulation of carbon catabolite repression in *Escherichia coli*. Microbiology 160 (6), 1214–1223.

Borisov, V.F., 2000. Fuller's phenomenon. J. Math. Sci. 100 (4), 2311–2354.

Caillau, Jean-Baptiste, Djema, Walid, Gouzé, Jean-Luc, Maslovskaya, Sofya, Pomet, Jean-Baptiste, 2022. Turnpike property in optimal microbial metabolite production. J. Optim. Theory Appl. 194 (2), 375–407.

Carlson, Dean A., Haurie, Alain B., Leizarowitz, Arie, 2012. Infinite Horizon Optimal Control: Deterministic and Stochastic Systems. Springer Science & Business Media.

Djema, Walid, Bayen, Térence, Bernard, Olivier, 2022. Optimal darwinian selection of microorganisms with internal storage. Processes 10 (3), 461.

Djema, Walid, Giraldi, Laëtitia, Maslovskaya, Sofya, Bernard, Olivier, 2021. Turnpike features in optimal selection of species represented by quota models. Automatica 132, 109804.

Edwards, Jeremy S., Ibarra, Rafael U., Palsson, Bernhard O., 2001. In silico predictions of *Escherichia coli* metabolic capabilities are consistent with experimental data. Nature Biotechnol. 19 (2), 125–130.

Ehrenberg, Mans, Bremer, Hans, Dennis, Patrick P., 2013. Medium-dependent control of the bacterial growth rate. Biochimie 95 (4), 643–658.

Ewald, Jan, Bartl, Martin, Kaleta, Christoph, 2017. Deciphering the regulation of metabolism with dynamic optimization: an overview of recent advances. Biochem. Soc. Trans. 45 (4), 1035–1043.

Gaca, Anthony O., Colomer-Winter, Cristina, Lemos, José A., 2015. Many means to a common end: the intricacies of (p) ppGpp metabolism and its control of bacterial homeostasis. J. Bacteriol. 197 (7), 1146–1156.

Giordano, Nils, et al., 2016. Dynamical allocation of cellular resources as an optimal control problem: novel insights into microbial growth strategies. PLoS Comput. Biol. 12 (3), e1004802.

Ibarra, Rafael U., Edwards, Jeremy S., Palsson, Bernhard O., 2002. *Escherichia coli* K-12 undergoes adaptive evolution to achieve in silico predicted optimal growth. Nature 420 (6912), 186–189.

Inria Saclay Team Commands, 2017. BOCOP: an open source toolbox for optimal control. See http://bocop.org.

Lewis, Nathan E., et al., 2010. Omic data from evolved *E. coli* are consistent with computed optimal growth from genome-scale models. Mol. Syst. Biol. 6 (1), 390.

Liao, James C., et al., 2016. Fuelling the future: microbial engineering for the production of sustainable biofuels. Nature Rev. Microbiol. 14 (5), 288–304.

Liu, Kuanqing, Bittner, Alycia N., Wang, Jue D., 2015. Diversity in (p) ppGpp metabolism and effectors. Curr. Opinion Microbiol. 24, 72–79.

Magnusson, Lisa U., Farewell, Anne, Nyström, Thomas, 2005. ppGpp: a global regulator in *Escherichia coli*. Trends Microbiol. 13 (5), 236–242.

Mairet, Francis, Bayen, Térence, 2021. The promise of dawn: microalgae photoacclimation as an optimal control problem of resource allocation. J. Theoret. Biol. 515, 110597.

Maitra, Arijit, Dill, Ken A., 2015. Bacterial growth laws reflect the evolutionary importance of energy efficiency. Proc. Natl. Acad. Sci. 112 (2), 406–411.

Marchal, Christian, 1973. Chattering arcs and chattering controls. J. Optim. Theory Appl. 11, 441–468.

Muratore, Daniel, et al., 2022. Complex marine microbial communities partition metabolism of scarce resources over the diel cycle. Nat. Ecol. Evol. 6 (2), 218–229.

Nguyen, Jen, Lara-Gutiérrez, Juanita, Stocker, Roman, 2021a. Environmental fluctuations and their effects on microbial communities, populations and individuals. FEMS Microbiol. Rev. 45 (4), fuaa068.

Nguyen, Jen, et al., 2021b. A distinct growth physiology enhances bacterial growth under rapid nutrient fluctuations. Nature Commun. 12 (1), 3662.

Pavlov, Michael Y., Ehrenberg, Mans, 2013. Optimal control of gene expression for fast proteome adaptation to environmental change. Proc. Natl. Acad. Sci. 110 (51), 20527–20532.

Potrykus, Katarzyna, Cashel, Michael, 2008. (p) ppGpp: still magical? Annu. Rev. Microbiol. 62, 35–51.

Potrykus, Katarzyna, et al., 2011. Ppgpp is the major source of growth rate control in *E. coli*. Environ. Microbiol. 13 (3), 563–575.

Scott, Matthew, et al., 2014. Emergence of robust growth laws from optimal regulation of ribosome synthesis. Mol. Syst. Biol. 10 (8), 747.

Silveston, P.L., Budman, H., Jervis, E., 2008. Forced modulation of biological processes: A review. Chem. Eng. Sci. 63 (20), 5089–5105.

Trélat, Emmanuel, 2023. Linear turnpike theorem. Math. Control Signals Syst. 35 (3), 685–739.

van den Berg, Hugo A., et al., 1998. Optimal allocation between nutrient uptake and growth in a microbial trichome. J. Math. Biol. 37, 28–48.

Waldherr, Steffen, Oyarzún, Diego A., Bockmayr, Alexander, 2015. Dynamic optimization of metabolic networks coupled with gene expression. J. Theoret. Biol. 365, 469–485.

Yabo, Agustín Gabriel, Caillau, Jean-Baptiste, Gouzé, Jean-Luc, 2024. Optimal bacterial resource allocation strategies in batch processing. SIAM J. Appl. Math. S567–S591.

Yabo, Agustín G., et al., 2022. Dynamical analysis and optimization of a generalized resource allocation model of microbial growth. SIAM J. Appl. Dyn. Syst. 21 (1), 137–165.

Yegorov, Ivan, et al., 2019. Optimal control of bacterial growth for the maximization of metabolite production. J. Math. Biol. 78, 985–1032.